

# Transitively Consistent and Unbiased Multi-Image Registration Using Numerically Stable Transformation Synchronisation

Florian Bernard<sup>1,2</sup>, Johan Thunberg<sup>2</sup>, Andreas Husch<sup>1,2</sup>, Luis Salamanca<sup>2</sup>,  
Peter Gemmar<sup>3</sup>, Frank Hertel<sup>1</sup> and Jorge Goncalves<sup>2,4</sup>

<sup>1</sup> Centre Hospitalier de Luxembourg, Luxembourg City, LUXEMBOURG

<sup>2</sup> Luxembourg Centre for Systems Biomedicine, University of Luxembourg,  
Esch-sur-Alzette, LUXEMBOURG

<sup>3</sup> Trier University of Applied Sciences, Trier, GERMANY

<sup>4</sup> Control Group, Department of Engineering, University of Cambridge, Cambridge,  
UNITED KINGDOM

**Abstract.** Transitive consistency of pairwise transformations is a desirable property of groupwise image registration procedures. The transformation synchronisation method [4] is able to retrieve transitively consistent pairwise transformations from pairwise transformations that are initially not transitively consistent. In the present paper, we present a numerically stable implementation of the transformation synchronisation method for affine transformations, which can deal with very large translations, such as those occurring in medical images where the coordinate origins may be far away from each other. By using this method in conjunction with any pairwise (affine) image registration algorithm, a transitively consistent and unbiased groupwise image registration can be achieved. Experiments involving the average template generation from 3D brain images demonstrate that the method is more robust with respect to outliers and achieves higher registration accuracy compared to reference-based registration.

**Keywords:** template construction, multi-image registration, groupwise registration, transformation synchronisation, multi-alignment.

## 1 Introduction

Image registration has attracted a lot of attention in the medical imaging community mainly due to the vast amount of applications both in research and in the clinic. Applications include surgery planning, multi-modal diagnosis, statistical analyses, normalisation, computational anatomy, longitudinal studies, image segmentation, and many more. The registration (or alignment) of a *moving image* with a *fixed image* can be defined as finding a spatial mapping that transforms the moving image such that it fits the fixed image “best”. To measure the agreement of two images, mostly intensity-based metrics are used as surrogates for the unknown true correspondence. The mapping is in general obtained by

optimisation methods, where it is necessary to select an application-dependent transformation model. Commonly, the transformation models are categorised by affine/linear and deformable transformations. Affine transformation models have a low number of degrees-of-freedom that allow only for a coarse alignment and thus are insensitive to overfitting. On the contrary, deformable transformation models are capable of aligning images on a very fine scale; however, controlling the trade-off between overfitting and realistic deformation is difficult. Frequently, affine transformations serve as initialisation for deformable transformations to avoid overfitting in the early stage of the optimisation.

The simultaneous registration of multiple images is more difficult. Different approaches to tackle this problem are: aligning each image individually to a *fixed reference* (e.g. chosen as one of the images); aligning each image with an iteratively *evolving reference image* [13, 15]; finding a *path of pairwise transformations* containing all images [17]; *image congealing*, where the variability along the known axes of variation is removed iteratively [14, 21], and the related *accumulated pair-wise estimates (APE)* approach [20]; considering a *minimum description length* (MDL) approach of a statistical shape model built from the correspondences given due to the groupwise image registration [5]; or, using a Bayesian formulation for dense template estimation based on *Expectation Maximisation* (EM) [1]. In [19], for video mosaicing with motion distortion correction, global alignment is seen as estimation problem on a Lie group.

However, choosing a fixed reference image or a path of sequential transformations induces a bias, and the iterative methods are generally local methods that are initialisation-dependent. In any case this may result in suboptimal alignments. One way of measuring the degree of suboptimality is to use a transitive consistency criterion, which is based on the fact that for a perfect alignment the composite transformation from A to B to C must be identical to the direct transformation from A to C. Registration methods improving this transitive consistency have been proposed for deformable transformations [8, 9].

Based on recent works on transformation synchronisation [4], in this paper an unbiased, truly reference-free and transitively consistent approach for aligning multiple images under the affine transformation model is presented. Our approach is useful in applications where the affine alignment of multiple images is required. This includes for example the creation of an affine average template, the creation of an (affine) probabilistic atlas, or the initialisation for deformable multi-image alignment. Furthermore, since our approach is unbiased, the resulting average template is attractive for statistical analyses. By exploiting redundancies between pairwise transformations, a more global approach of multi-image registration is achieved with the proposed method. Compared to reference-based groupwise registration, this leads to higher registration accuracy.

## 2 Methods

In this section, the transformation synchronisation method is briefly recapitulated and a numerically stable implementation thereof is presented that can

handle large translations. Subsequently it is described how the method can be applied to multi-image registration.

## 2.1 Overview of Transformation Synchronisation

Transformation synchronisation is a method for reconstructing transitively consistent transformations from the set of (disturbed) pairwise transformations [4], which is briefly summarised in the following.

At first, the case of perfect (undisturbed) data is described. Given is the set  $\mathcal{T} = \{T_{ij}\}_{i,j=1}^k$  containing  $k^2$  pairwise transformations, where  $T_{ij} \in \mathbb{R}^{4 \times 4}$  denotes an invertible affine 3D transformation matrix from image  $i$  to image  $j$  represented in homogeneous coordinates. The set  $\mathcal{T}$  is said to be transitively consistent if  $T_{ij}T_{jl} = T_{il}$  holds for all  $i, j, l = 1, \dots, k$ .

Assuming transitive consistency, every transformation matrix  $T_{ij}$  can be represented as  $T_{i\star}T_{\star j}$ , where  $\star$  denotes *some* reference coordinate system that is fixed for all  $i, j = 1, \dots, k$  (see [4]). For the case of undisturbed data, for any  $l$  it also holds that  $T_{\star l} = T_{l\star}^{-1}$ . Arranging all  $k^2$  transformations into a  $4k \times 4k$  matrix  $W$  gives

$$W = \begin{bmatrix} T_{11} & \cdots & T_{1k} \\ \vdots & \ddots & \vdots \\ T_{k1} & \cdots & T_{kk} \end{bmatrix} = [T_{ij}] = [T_{i\star}T_{\star j}] = [T_{i\star}T_{j\star}^{-1}] = U_1U_2, \quad (1)$$

with  $U_1 = [T_{1\star}^T T_{2\star}^T \dots T_{k\star}^T]^T$  and  $U_2 = [T_{1\star}^{-1}, T_{2\star}^{-1}, \dots, T_{k\star}^{-1}]$ . This shows that for transitively consistent transformations the matrix  $W$  can be factorised into  $U_1U_2$ .

Multiplying (1) with  $U_1$  from the right leads to  $WU_1 = U_1U_2U_1$ . Considering now that  $U_2U_1 = k\mathbf{I}_4$ , where  $\mathbf{I}_n$  denotes the  $n \times n$  identity matrix, this results in

$$WU_1 = kU_1 \quad \Leftrightarrow \quad ZU_1 = \mathbf{0}_{4k \times 4} \text{ with } Z = W - k\mathbf{I}_{4k}. \quad (2)$$

The latter shows that  $U_1$  can, up to an invertible linear transformation multiplied on the right, be obtained by finding the 4-dimensional nullspace of  $Z$ .

Now, if the pairwise transformations are obtained by independent measurements (e.g. pairwise image registrations), in general it does not hold that the transformations are transitively consistent or inverse consistent. Therefore, in general  $Z$  does not have a 4-dimensional nullspace. Instead, we consider the least-squares approximation of the 4-dimensional nullspace of  $Z$ , which can be obtained by singular value decomposition (SVD) of  $Z$ . Let  $\bar{W} = [\bar{T}_{ij}] = U_1U_2$  be the so-obtained synchronised version from a noisy  $W = [T_{ij}]$ .

## 2.2 Numerical Stability for Large Translations

Large translations in the pairwise transformations may lead to an ill-posed matrix  $W$ , constituting a problem with respect to the numerical stability of the synchronisation method.

Each affine transformation block  $T_{ij}$  in  $W$  has the form

$$T_{ij} = \begin{bmatrix} A_{ij} & \mathbf{0}_{3 \times 1} \\ t_{ij} & 1 \end{bmatrix} \text{ with } A_{ij} \in \mathbb{R}^{3 \times 3} \text{ and } t_{ij} \in \mathbb{R}^{1 \times 3}. \quad (3)$$

Generally, in medical image registration it can be assumed that the anatomical entities depicted in the images are similar to a certain extent as they represent objects of the same (fixed) class (e.g. brains). This imposes certain properties onto the linear part  $A_{ij}$  of the transformation: the rotational part of  $A_{ij}$  can be arbitrary, because in principal the orientation of the patient can be arbitrary. In contrast, the scaling or shearing are not arbitrary (for example it is unlikely that the scale between two individual adult brains differs by a factor of 10 or even more). Both properties imply that the values of the elements in  $A_{ij}$  are bounded, i.e. they are in (or close to) the interval  $[-1, 1]$ . In contrast, the origin of the coordinate frame of each image can, in principal, be arbitrary. With that, the values of the elements in the translation component  $t_{ij}$  do not have such a bound, i.e. they can be orders of magnitude larger than the elements of the linear part, which impairs numerical stability.

Instead of directly finding the 4-dimensional least-squares approximation of the nullspace of  $Z = W - k\mathbf{I}_{4k}$ , a numerically more stable approach is now described. For affine transformations  $T_{ij}$  the matrix  $Z$  is reducible, i.e. for some permutation matrix  $P$ , the matrix  $Z' = P^T Z P$  is a block upper triangular matrix of the form

$$Z' = P^T Z P = \begin{bmatrix} Z_{11} & Z_{12} \\ \mathbf{0}_{3k \times k} & Z_{22} \end{bmatrix}, \quad (4)$$

where the lower left block  $\mathbf{0}_{3k \times k}$  contains the zeros from the homogeneous transformation part,  $Z_{11} \in \{1, 1-k\}^{k \times k}$  contains the constant elements from the homogeneous transformation part,  $Z_{22} \in \mathbb{R}^{3k \times 3k}$  contains the linear transformation part, and  $Z_{12} \in \mathbb{R}^{k \times 3k}$  contains the (possibly large) translation components. Using the Dulmage-Mendelsohn decomposition [7], the permutation  $P$  transforming  $Z$  to  $Z'$  in (4) is determined. In the following it is described how  $U'_1$ , spanning the 4-dimensional nullspace of  $Z'$ , can be obtained. From  $U'_1$ , the matrix  $U_1$  can directly be obtained by  $U_1 = PU'_1$ .

Writing  $U'_1 \in \mathbb{R}^{4k \times 4}$  as  $U'_1 = [V_1^T \ V_2^T]^T$ , where  $V_1 \in \mathbb{R}^{k \times 4}$  and  $V_2 \in \mathbb{R}^{3k \times 4}$ , allows to rewrite eq. (2) for  $Z'$  as

$$Z' U'_1 = \mathbf{0}_{4k \times 4} \quad \Leftrightarrow \quad \begin{bmatrix} Z_{11} & Z_{12} \\ \mathbf{0}_{3k \times k} & Z_{22} \end{bmatrix} \begin{bmatrix} V_1 \\ V_2 \end{bmatrix} = \mathbf{0}_{4k \times 4}. \quad (5)$$

Eq. (5) is solved first for the matrix  $V_2$  by finding the 4-dimensional nullspace of  $Z_{22}$  using singular value decomposition, which is stable since  $Z_{22}$  contains the (well-posed) linear transformation parts only. Once  $V_2$  is known, the remaining part  $V_1$  of  $U'_1$  is determined by solving the linear system of equations  $Z_{11}V_1 = -Z_{12}V_2$  for  $V_1$ . Obtaining  $U_1$  from  $U'_1$ ,  $U_2$  from  $U_1$ , and reconstructing  $\bar{W} = U_1 U_2$  eventually gives the synchronised version  $\bar{W}$  of  $W$ .

### 2.3 Multi-image Alignment

The processing pipeline of aligning multiple images is illustrated in Fig. 1.

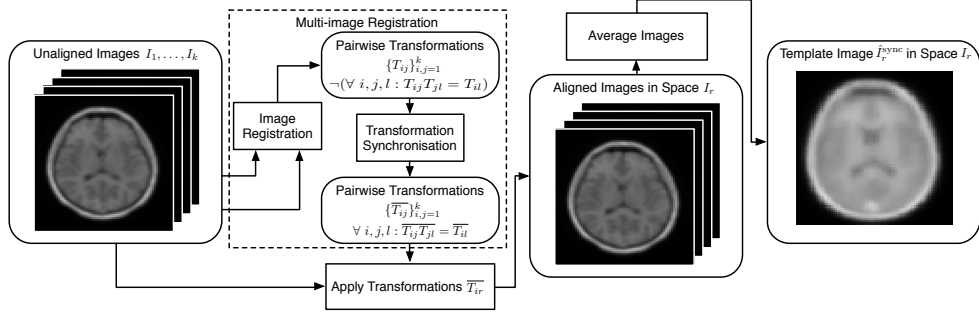


**Fig. 1.** Processing pipeline for aligning multiple images using transformation synchronisation. Rectangles represent *methods* and rounded rectangles represent *data*.

First the set of transformations  $\{T_{ij}\}_{i,j=1}^k$  between all pairs of unaligned images  $I_1, \dots, I_k$  is determined using any affine image registration algorithm. Then, all transformations are synchronised using the numerically stable synchronisation method, resulting in the set  $\{\bar{T}_{ij}\}_{i,j=1}^k$  of transitively consistent pairwise transformations.

In order to represent all images in the *same* coordinate system it is necessary to select such a common coordinate system. Due to the transitive consistency of the set of all pairwise transformations, in theory it is irrelevant what is chosen as common coordinate system. To be more specific, up to discretisation and interpolation, the resulting average image is the same for *any* choice of coordinate system, thus, we consider our approach to be *unbiased*. Interpolation bias can for example be handled by a mid-space based normalisation [15].

In order to be able to directly compare our method to the reference-based approach, we create average images with the common coordinate system, image dimension and voxel size of image  $I_r$  for all  $r = 1, \dots, k$ . So, for a given image  $I_r$ , each image  $I_i$  (for  $i = 1, \dots, k$ ) is transformed to the space of the image  $I_r$  by applying the transformation  $T_{ir}$ . We emphasize that  $I_r$  should not be confused with the reference image in reference-based multi-image registration (cf. preceding paragraph). Eventually, the average image  $\hat{I}_r^{\text{sync}}$  of all  $k$  images (represented in the space of  $I_r$ , thus having the same image dimensions) is computed.

The use of transformation synchronisation constitutes the major difference to reference-based template creation approaches, since this method is able to aggregate *all* information contained in the set of pairwise transformations, in contrast to reference-based methods, which only incorporate the information contained in  $k$  pairwise transformations.

## 3 Experiments

In this section the results of applying the proposed framework for the unbiased template construction from 17 T1-weighted MR images is described. The dimen-

sions of the images are between  $256 \times 256 \times 122$  and  $512 \times 512 \times 168$  voxels, where the voxel sizes vary from  $0.5 \times 0.5 \times 1$  to approximately  $0.9 \times 0.9 \times 1.4$  (in mm<sup>3</sup>).

Two different affine registration methods have been used to find the set of pairwise transformations (FLIRT [11] and ANTS [2]). To run the FLIRT algorithm, we set parameters as follows: normalised mutual information, 12 degrees-of-freedom and search angle  $[-20, 20]$  for the rotation in all directions. Cross-correlation and the affine transformation model were used in ANTS. Other parameters remained unchanged.

The reference-based alignment of images is used as baseline: (i) selection of reference image  $I_r$ ; (ii) registration of all other images with  $I_r$ ; (iii) transformation of all images to space of  $I_r$ ; and (iv) computation of average template  $\hat{I}_r^{\text{ref}}$ . In order to perform a fair analysis the evaluation has been carried out for all  $r = 1, \dots, k$  images  $I_r$  as reference.

Furthermore, to enable a direct comparison between the reference-based and synchronisation-based methods, for the latter a total of  $k$  average template images  $\hat{I}_1^{\text{sync}}, \dots, \hat{I}_k^{\text{sync}}$  are created. The results of the synchronisation-based method are represented in the image spaces  $I_r$  for  $r = 1, \dots, k$  only for the sake of comparability with the reference-based method. By representing image  $I_i$  in the space of image  $I_r$  we mean applying the respective transformations, i.e.  $T_{ir}$  for the reference-based method and  $\overline{T_{ir}}$  for the synchronisation-based method.

The average transitivity error  $e_{\text{trans}}(\mathcal{T})$  of a set of transformations  $\mathcal{T} = \{T_{ij}\}_{i,j=1}^k$ , which measures the degree of transitive consistency of the set of pairwise transformations  $\mathcal{T}$ , is defined as

$$e_{\text{trans}}(\mathcal{T}) = \frac{1}{k^3} \sum_{i,j,l=1}^k \|T_{ij}T_{jl} - T_{il}\|_F, \quad (6)$$

where  $\|\cdot\|_F$  denotes the Frobenius norm.

Let  $ncc(I_i, I_j)$  be the normalised cross-correlation (NCC) between the images  $I_i$  and  $I_j$ . In each experiment the NCC is computed  $k^2$  times, i.e. for all  $r = 1, \dots, k$  and  $i = 1, \dots, k$  the NCC is evaluated. For the reference-based method the NCC is computed as  $c_{ir}^{\text{ref}} = ncc(I_i, \hat{I}_r^{\text{ref}})$ , and for the synchronisation-based method as  $c_{ir}^{\text{sync}} = ncc(I_i, \hat{I}_r^{\text{sync}})$ , where image  $I_i$  is in both cases represented in the space of  $I_r$ .

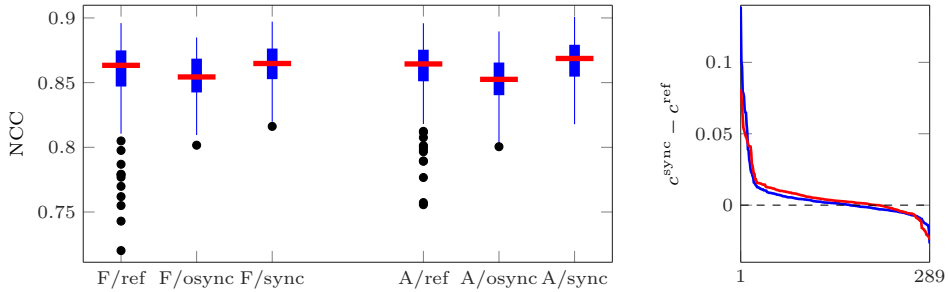
Additionally to the average transitivity error and NCC, a landmark-based evaluation criterion has been used. Based on a total of 8 bilateral brain structure segmentations of *subthalamic nucleus* & *substantia nigra* (as compound object), *nucleus ruber*, *putamen* & *globus pallidus* (as compound object), and *thalamus* [3], the centre of gravity (COG) of each segmented object is determined. Let  $e_{o,i,j,r}$  be the *cog-error* that is defined as the magnitude of the error vector between the COG of object  $o$  in image  $I_i$  and the COG of object  $o$  in image  $I_j$ , where  $I_i$  and  $I_j$  are both represented in the space of image  $I_r$ . In each experiment the cog-error is computed  $8k^3$  times for all  $r = 1, \dots, k$ ;  $i = 1, \dots, k$ ;  $j = 1, \dots, k$  and for all eight objects  $o = 1, \dots, 8$ .

Results for the measures described above are summarised in Table 1.

	$e_{\text{trans}}^{\text{ref}}$	$e_{\text{trans}}^{\text{sync}}$	$c^{\text{ref}}$	$c^{\text{sync}}$	$e^{\text{ref}}$	$e^{\text{sync}}$
F	9.142	<b>0</b>	$0.859 \pm 0.025$	<b><math>0.863 \pm 0.017</math></b>	$5.042 \pm 3.672$	<b><math>4.362 \pm 2.439</math></b>
A	12.004	<b>0</b>	$0.861 \pm 0.022$	<b><math>0.867 \pm 0.017</math></b>	$5.157 \pm 4.062$	<b><math>4.394 \pm 2.483</math></b>

**Table 1.** Comparison of reference-based method and synchronisation-based method for two experiments (F=FLIRT, A=ANTS). The scores shown are the average transitivity errors  $e_{\text{trans}}^{\{\text{ref},\text{sync}\}}$  (high values indicate problems), the mean and the standard deviation of the NCC  $c^{\{\text{ref},\text{sync}\}}$  (higher mean is better), and the mean and the standard deviation of the cog-error  $e^{\{\text{ref},\text{sync}\}}$  in mm (lower is better).

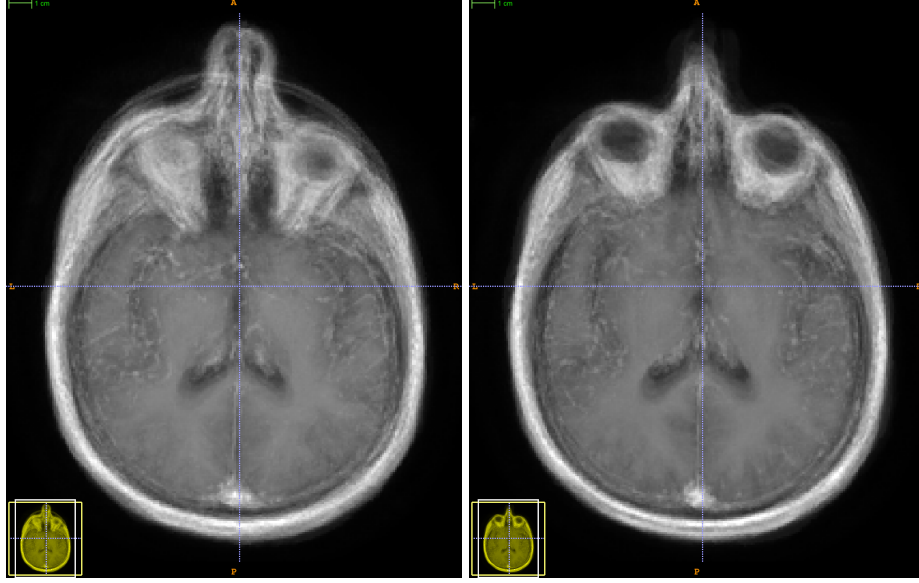
For both experiments the distributions of  $c_{ir}^{\{\text{ref},\text{osync},\text{sync}\}}$  and  $e_{o,i,j,r}^{\{\text{ref},\text{osync},\text{sync}\}}$  are presented as boxplots in Fig. 2 and 4, where the superscripts *osync* and *sync* are used to distinguish the original transformation synchronisation method and our proposed transformation synchronisation method with the numerical stability improvement.



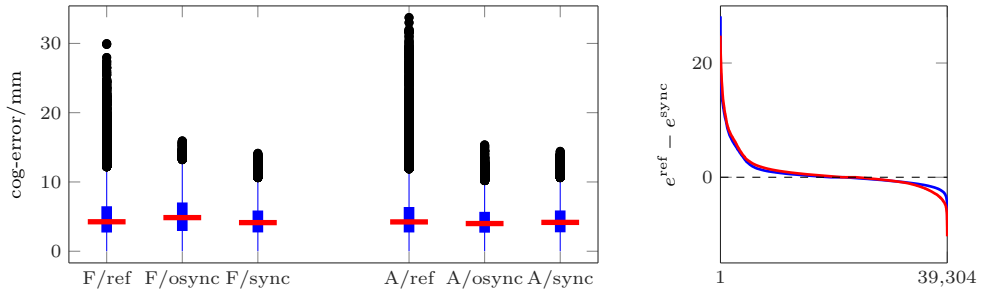
**Fig. 2.** Left: distribution of NCC  $c_{ir}$  for  $i = 1, \dots, k$  and  $r = 1, \dots, k$  for the reference-based method and the synchronisation-based methods (with and without the numerical stability improvement) visualised as boxplots (median as red horizontal line, 25th and 75th percentile as blue box, extent of extreme points that are not considered outliers as blue vertical line and outliers as black dots). Right: sorted NCC differences  $c_{ir}^{\text{sync}} - c_{ir}^{\text{ref}}$  for  $i = 1, \dots, k$  and  $r = 1, \dots, k$  (FLIRT in blue, ANTS in red).

Fig. 2 reveals that with respect to NCC, on average the proposed approach outperforms the reference-based method, whereas the original transformation synchronisation method without the numerical stability improvement delivers on average lower scores than both the reference-based method and our proposed method. Furthermore, the boxplots show that using the reference-based method may result in outliers that have considerably lower NCC scores. Fig. 3 (left) shows such a case when using the reference-based method for brain average template creation, where there are undesired artefacts in the area of the nose that are not present using the proposed synchronisation method (right).

Considering transitive consistency, which is frequently employed for evaluating the quality of registration methods [6, 8, 10], the proposed approach significantly outperforms the reference-based method since our method always results in perfect transitive consistency. Whilst a low average transitivity error does not necessarily imply a good registration (e.g. consider the trivial case of not per-



**Fig. 3.** Axial slices of brain average templates created using the reference-based method (left) and the proposed synchronisation-based approach (right). Note the “ghost effect” in the area of the nose for the reference-based method stemming from a bad registration.



**Fig. 4.** Left: distribution of the cog-error  $e_{o,i,j,r}$  for  $i = 1, \dots, k$ ;  $j = 1, \dots, k$ ;  $r = 1, \dots, k$  and  $o = 1, \dots, 8$  for the reference-based method and the synchronisation-based methods (with and without the numerical stability improvement) visualised as boxplots (median as red horizontal line, 25th and 75th percentile as blue box, extent of extreme points that are not considered outliers as blue vertical line and outliers as black dots). Right: sorted cog-error differences  $e_{o,i,j,r}^{\text{ref}} - e_{o,i,j,r}^{\text{sync}}$  for  $i = 1, \dots, k$ ;  $j = 1, \dots, k$ ;  $r = 1, \dots, k$  and  $o = 1, \dots, 8$  (FLIRT in blue, ANTS in red).

forming a registration at all, i.e. setting all transformations to identity), a large average transitivity error indicates that there is a problem with the registration.

The cog-error, shown as boxplots in Fig. 4, reveal some extreme outliers of up to around 3.5 cm when using the reference-based method. For the synchronisation-based methods the cog-error is always below 2 cm, where the proposed synchronisation method with the numerical stability improvement has a slightly lower median when using FLIRT for finding the pairwise transformations than the

original synchronisation method. Note that in general the cog-errors have comparably large values since due to the regularity of the affine transformation model only a coarse alignment of structures is possible.

## 4 Conclusion

A solution for the groupwise affine registration of images based on transformation synchronisation has been presented. It has been shown that the method is more robust with respect to outliers than the common reference-based method and that it leads to improved registration accuracy. Our proposed approach can be seen as an averaging procedure that removes noise (accounting for transitive inconsistency) from pairwise transformations.

A shortcoming is that a quadratic number of pairwise transformations needs to be available, which may, depending on the application, be unaffordable. However, because an average template is usually created only once, in many cases the computational overhead may be acceptable, since the extra-effort is compensated by a more reliable result. An alternative approach is to find a trade-off between complete unbiasedness and computational cost by synchronising only a subset of all pairwise transformations using transformation synchronisation for partial data [18].

On its own, the proposed affine groupwise image registration procedure is valuable for the construction of affine average templates. Moreover, it can be used as initialisation for groupwise deformable image registration, where a good initial solution is essential due to the highly non-convex nature of deformable registration methods. In [12] a hierarchical groupwise registration scheme is presented that already assumes a groupwise affine registration between all images. Also, in [16], for brain template generation the affine registration of a set of images is performed by registering all images to an existing average template. In both approaches our method can be used for the groupwise affine registration.

Due to the unbiasedness of the method it is ideal for statistical analyses. Our experiments suggest that the reference-based method performs significantly worse for certain choices of reference images, rendering the choice of reference crucial. Since a priori it is unknown which of the images is a good reference and which is not, a reference-free method is favourable in many scenarios.

## Acknowledgements

This work is supported by the Fonds National de la Recherche, Luxembourg (5748689, 6538106, 8864515, 9169303).

## References

1. Allouanière, S., Amit, Y., Trouvé, A.: Towards a coherent statistical framework for dense deformable template estimation. *Journal of the Royal Statistical Society: Series B (Statistical Methodology)* 69(1), 3–29 (2007)

2. Avants, B.B., Tustison, N.J., Song, G., Cook, P.A., Klein, A., Gee, J.C.: A reproducible evaluation of ANTs similarity metric performance in brain image registration. *Neuroimage* 54(3), 2033–2044 (2011)
3. Bernard, F., Gemmar, P., Husch, A., Saleh, C., Neb, H., Doomes, G., Hertel, F.: Improving the Consistency of Manual Deep Brain Structure Segmentations by Combining Variational Interpolation, Simultaneous Multi-Modality Visualisation and Histogram Equilisation. *Biomed Tech* (59 (Suppl. 1)) (Oct 2014)
4. Bernard, F., Thunberg, J., Gemmar, P., Hertel, F., Husch, A., Goncalves, J.: A Solution for Multi-Alignment by Transformation Synchronisation. In: *CVPR* (Jun 2015)
5. Cootes, T.F., Marsland, S., Twining, C.J., Smith, K., Taylor, C.J.: Groupwise diffeomorphic non-rigid registration for automatic model building. In: *ECCV*, pp. 316–327. Springer (2004)
6. Datteri, R.D., Dawant, B.M.: Automatic detection of the magnitude and spatial location of error in non-rigid registration. In: *Biomedical Image Registration*, pp. 21–30. Springer (2012)
7. Dulmage, A.L., Mendelsohn, N.S.: Coverings of bipartite graphs. *Canadian Journal of Mathematics* 10(4), 516–534 (1958)
8. Gass, T., Székely, G., Goksel, O.: Detection and Correction of Inconsistency-based Errors in Non-Rigid Registration. In: *SPIE Medical Imaging*. p. 90341B (Feb 2014)
9. Geng, X.: Transitive Inverse-consistent Image Registration and Evaluation. PhD thesis (2007)
10. Holden, M., Hill, D.L., Denton, E.R., Jarosz, J.M., Cox, T.C., Rohlfing, T., Goodey, J., Hawkes, D.J.: Voxel similarity measures for 3-D serial MR brain image registration. *TMI* 19(2), 94–102 (Feb 2000)
11. Jenkinson, M., Smith, S.: A global optimisation method for robust affine registration of brain images. *MedIA* 5(2), 143–156 (Jun 2001)
12. Jia, H., Wu, G., Wang, Q., Shen, D.: ABSORB: Atlas building by self-organized registration and bundling. *Neuroimage* 51(3), 1057–1070 (2010)
13. Joshi, S., Davis, B., Jomier, M., Gerig, G.: Unbiased diffeomorphic atlas construction for computational anatomy. *Neuroimage* 23 Suppl 1, S151–60 (2004)
14. Learned-Miller, E.G.: Data driven image models through continuous joint alignment. *TPAMI* 28(2), 236–250 (Feb 2006)
15. Reuter, M., Schmansky, N.J., Rosas, H.D., Fischl, B.: Within-subject template estimation for unbiased longitudinal image analysis. *Neuroimage* 61(4), 1402–1418 (2012)
16. Seghers, D., D'Agostino, E., Maes, F., Vandermeulen, D., Suetens, P.: Construction of a brain template from MR images using state-of-the-art registration and segmentation techniques. In: *MICCAI*, pp. 696–703. Springer (2004)
17. Škrinjar, O., Bistoquet, A., Tagare, H.: Symmetric and Transitive Registration of Image Sequences. *International Journal of Biomedical Imaging* 2008, 1–9 (2008)
18. Thunberg, J., Bernard, F., Goncalves, J.: On Transitive Consistency for Linear Invertible Transformations between Euclidean Coordinate Systems. *arXiv:1509.00728* (2015)
19. Vercauteren, T., Perchant, A., Malandain, G., Pennec, X., Ayache, N.: Robust mosaicing with correction of motion distortions and tissue deformations for in vivo fibered microscopy. *MedIA* 10(5), 673–692 (Oct 2006)
20. Wachinger, C., Navab, N.: Simultaneous registration of multiple images: similarity metrics and efficient optimization. *TPAMI* 35(5), 1221–1233 (May 2013)
21. Zöllei, L., Learned-Miller, E., Grimson, E., Wells, W.: Efficient population registration of 3D data. In: *Computer Vision for Biomedical Image Applications*, pp. 291–301. Springer (2005)